

# Development of a 4-DOF SCARA Robot with 3R1P for Pick-and-Place Tasks

Wen-Bo Li<sup>1</sup> Guang-Zhong Cao<sup>1</sup> Xiao-Qin Guo<sup>1</sup> Su-Dan Huang<sup>1,2</sup>

<sup>1</sup> Shenzhen Key Laboratory of Electromagnetic Control, Shenzhen University, Shenzhen, China

E-mail: liwenbochn@126.com; gzcao@szu.edu.cn; guoxq@szu.edu.cn;

<sup>2</sup> College of Electrical Engineering, Southwest Jiaotong University, Chengdu, 610031, China

E-mail: hdsudan@gmail.com

**Abstract**—The planar robot is very suitable for moving workpieces which are in high demand in industrial automation. This paper develops a 4 degree of freedom (4-DOF) selective compliance assembly robot arm (SCARA) robot with three rotary joints and one prismatic joint (3R1P) to realize pick-and-place tasks of the circular and rectangular workpieces. The structure of the robot is firstly presented. The kinematic model is then built, and the kinematic analysis is performed based on MATLAB. The trajectory planning is further implemented. A control interface is also designed via Visual C++ to control the robot for achieving pick-and-place tasks. The validity of the developed robot is finally verified through experimental results.

**Keywords**—Modeling, OpenCV, trajectory planning, SCARA, visual servoing.

## I. INTRODUCTION

Planar robots play an increasingly important role in industrial automation, especially in the assembly industry. Industrial planar robots are developed for fast, accurate, and repetitive tasks [1]. As one kind of the planar robot, the selective compliance assembly robot arm (SCARA) robot is pliable in planar and rigid in Z axis. The SCARA robot features simpler structure, lighter mass, faster response, more precise positioning accuracy compared to most of robots. Thus, the SCARA robot is widely applied to assembly industry. Additionally, pick-and-place tasks are basic operation of assembly processes, such as inserting an edge connector socket [2] into a printed circuit board, and classifying workpieces of sorting systems [3]. Currently, one of the world's fastest SCARA robots is Adept 1. Adept 1 has several times of velocity of other joints robots, which can reach 10 m/s of the end effector and achieve less than  $\pm 0.02$  mm repeated accuracy. The research of the SCARA robot focuses on accurate modeling [4], visual servo [5], human-robot collaboration [6], and trajectory planning [7], etc. In this paper, a 4 degree of freedom (4-DOF) SCARA robot with three rotary joints and one prismatic joint (3R1P) is developed for pick-and-place tasks by using visual servo control.

This paper is organized as follows. The hardware of the SCARA robot is presented in Section II. In Section III, the kinematic model of the SCARA robot is derived with the denavit-hartenberg (D-H) method, and the forward kinematic and inverse kinematic [8] are analyzed based on MATLAB. In Section IV, a straight line and an arc line for trajectory motion are planned in joint coordinates via Robotics Toolbox of MATLAB [9]. Section V discusses how to locate workpieces for pick up tasks by using position from visual servo. Conclusion remarks are given in Section VII.

## II. SYSTEM STRUCTURE

The prototype of the 4-DOF SCARA robot with 3R1P is shown in Fig. 1. Axis 1, 2 and 4 are the rotational joints, and Axis 3 is the prismatic joint. An Electromagnet clamp is installed on Axis 4, which is applied as the end effector. And a camera is installed on the electromagnet clamp.

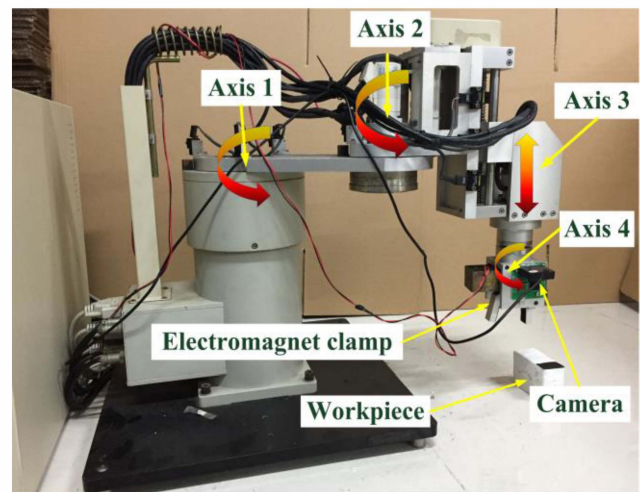


Fig. 1: Prototype of the 4-DOF SCARA robot with 3R1P

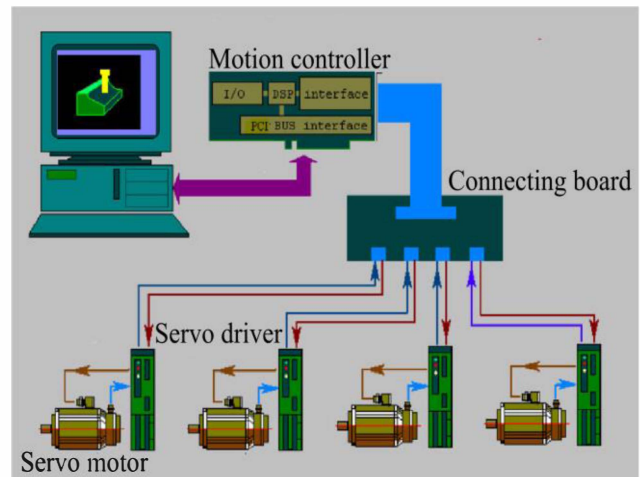


Fig. 2: Connection schematic diagram

Fig. 2 presents the connection of each part of the system. Each axis is driven by a Panasonic alternating current (AC) servo motor controlled by its Servo Driver. The parameters of the AC servo motor are given in Table 1. The PC+DSP control method is used in this system, and it is one of the most efficient methods to control robots in assembly industry. A Motion controller is installed on PC using PCI bus interface, its core is composed of an ADSP2181 DSP and a FPGA, and it can realize high-efficient calculation for control.

**Table 1: Parameters of the AC servo motor**

Parameters	Value
Input	3Φ AC 42 V 1.0 A
Rated output	0.05 KW
Rated frequency	200 Hz
Rated REV	3000 r/min

### III. KINEMATIC MODEL

Kinematic Modeling is analyzed in this section, and it consists of forward and inverse kinematic modeling. The D-H parameters of the robot are listed in the Table 2.

**Table 2: D-H parameters of the SCARA robot**

Axis	$\theta$	$d$	$a$	$\alpha$	Range
1	$\theta_1$	0	$l_1=200$ mm	0	$-10^\circ \sim 109^\circ$
2	$\theta_2$	0	$l_2=200$ mm	0	$-8^\circ \sim 102^\circ$
3	0	$d_3$	0	0	$-48$ mm $\sim 48$ mm
4	$\theta_4$	0	0	0	$-180^\circ \sim 180^\circ$

#### 1. Forward kinematic

When the robot movement of each joint is known, the process to solve the pose of the end effector is denoted as the forward kinematic of the robot. The D-H transformation matrix between link  $i-1$  and  $i$  is represented as (1). For the SCARA robot, after confirm the link coordinate, the transformation matrix from base coordinate to Axis 4 can be obtained and given in (2).

$$T_i = \begin{bmatrix} \cos \theta_i & -\sin \theta_i \cos \alpha_i & \sin \theta_i \sin \alpha_i & a_i \cos \theta_i \\ \sin \theta_i & \cos \theta_i \cos \alpha_i & -\cos \theta_i \sin \alpha_i & a_i \sin \theta_i \\ 0 & \sin \alpha_i & \cos \alpha_i & d_i \\ 0 & 0 & 0 & 1 \end{bmatrix} \quad (1)$$

$${}^0T_4 = {}^0T_1 {}^1T_2 {}^2T_3 {}^3T_4 \quad (2)$$

where  ${}^{i-1}T_i$  is the transformation matrix from coordinate  $n$  to  $m$ . Substituting D-H parameters into (1), the transformation matrix between links can be expressed as

$${}^0T_1 = \begin{bmatrix} \cos \theta_1 & -\sin \theta_1 & 0 & l_1 \cos \theta_1 \\ \sin \theta_1 & \cos \theta_1 & 0 & l_1 \sin \theta_1 \\ 0 & 0 & 1 & 0 \\ 0 & 0 & 0 & 1 \end{bmatrix} \quad (3)$$

$${}^1T_2 = \begin{bmatrix} \cos \theta_2 & \sin \theta_2 & 0 & l_2 \cos \theta_2 \\ \sin \theta_2 & -\cos \theta_2 & 0 & l_2 \sin \theta_2 \\ 0 & 0 & 1 & 0 \\ 0 & 0 & 0 & 1 \end{bmatrix} \quad (4)$$

$${}^2T_3 = \begin{bmatrix} 1 & 0 & 0 & 0 \\ 0 & 1 & 0 & 0 \\ 0 & 0 & 1 & d_3 \\ 0 & 0 & 0 & 1 \end{bmatrix} \quad (5)$$

$${}^3T_4 = \begin{bmatrix} \cos \theta_4 & -\sin \theta_4 & 0 & 0 \\ \sin \theta_4 & \cos \theta_4 & 0 & 0 \\ 0 & 0 & 1 & 0 \\ 0 & 0 & 0 & 1 \end{bmatrix} \quad (6)$$

Substituting (3), (4), (5), and (6) into (2), the transformation matrix of the end effector coordinate can be represented as

$${}^0T_4 = \begin{bmatrix} \cos(\theta_1 + \theta_2 - \theta_4) & \sin(\theta_1 + \theta_2 - \theta_4) & 0 & l_1 \cos(\theta_1) + l_2 \cos(\theta_1 + \theta_2) \\ \sin(\theta_1 + \theta_2 - \theta_4) & -\cos(\theta_1 + \theta_2 - \theta_4) & 0 & l_1 \sin(\theta_1) + l_2 \sin(\theta_1 + \theta_2) \\ 0 & 0 & 1 & d_3 \\ 0 & 0 & 0 & 1 \end{bmatrix} \quad (7)$$

According to the kinematic theory of robots, the solution of kinematic can be given by

$$\begin{cases} n_x = \cos(\theta_1 + \theta_2 - \theta_4) \\ n_y = \sin(\theta_1 + \theta_2 - \theta_4) \\ n_z = 0 \\ o_x = \sin(\theta_1 + \theta_2 - \theta_4) \\ o_y = \cos(\theta_1 + \theta_2 - \theta_4) \\ o_z = 0 \\ a_x = 0 \\ a_y = 0 \\ a_z = 1 \\ p_x = l_1 \cos(\theta_1) + l_2 \cos(\theta_1 + \theta_2) \\ p_y = l_1 \sin(\theta_1) + l_2 \sin(\theta_1 + \theta_2) \\ p_z = d_3 \end{cases} \quad (8)$$

#### 2. Inverse kinematic

In most situations, the movement of each joint from point A to point B is required. Inverse kinematic analysis is employed to solve this problem. There are two methods to solve the inverse kinematic problem, which are the closed-form solution and numerical solution [10]. However, in practice, due to the iterative of the numerical solution, the efficient of the numerical solution is less than closed-form solution. Therefore, the closed-form solution is chosen for the inverse kinematic.

$$({}^0T_1)^{-1} {}^0T_4 = {}^1T_2 {}^2T_3 {}^3T_4 \quad (9)$$

$$\begin{bmatrix} \cos \theta_1 & \sin \theta_1 & 0 & -l_1 \\ -\sin \theta_1 & \cos \theta_1 & 0 & 0 \\ 0 & 0 & 1 & 0 \\ 0 & 0 & 0 & 1 \end{bmatrix} \begin{bmatrix} n_x & o_x & a_x & p_x \\ n_y & o_y & a_y & p_y \\ n_z & o_z & a_z & p_z \\ 0 & 0 & 0 & 1 \end{bmatrix} = \begin{bmatrix} \cos(\theta_2 + \theta_4) & \sin(\theta_2 + \theta_4) & 0 & l_2 \cos \theta_2 \\ \sin(\theta_2 + \theta_4) & -\cos(\theta_2 + \theta_4) & 0 & l_2 \sin \theta_2 \\ 0 & 0 & 1 & d_3 \\ 0 & 0 & 0 & 1 \end{bmatrix} \quad (10)$$

The closed-form solution can be divided into the algebraic method and geometric method in terms of the solve method. Because the SCARA robot has relatively simple configuration, so the algebraic method is used. Equation (2) can be deformed as (9), compared the elements on both sides of (10), the solution of inverse kinematic can be derived as

$$\begin{cases} \theta_1 = \arctan\left(\frac{A}{\pm\sqrt{1-A^2}}\right) - \phi \\ \theta_2 = \arccos\left(\frac{r \sin(\theta_1 + \phi) - l_1}{l_2}\right) \\ d_3 = p_z \\ \theta_4 = \arcsin(n_y \cos(\theta_1) - n_x \sin(\theta_1)) - \theta_2 \\ A = \frac{l_1^2 + p_x^2 + p_y^2 - l_2^2}{2l_1\sqrt{p_x^2 + p_y^2}} \\ \phi = \arctan\left(\frac{p_x}{p_y}\right) \\ r = \sqrt{p_x^2 + p_y^2} \end{cases} \quad (11)$$

### 3. Modeling based on MATLAB

The Robotics Toolbox of MATLAB is developed by Professor Peter Corke. It provides a series function of kinematic and path planning to research of robots, and it is widely applied in the robot development. Meanwhile, the toolbox can also perform the image simulation based on robots. In Robotics Toolbox, it is important to construct the joints model. Function Link and SerialLink can be used in modeling. Fig. 3 illustrates the simulation model in 3-D space.

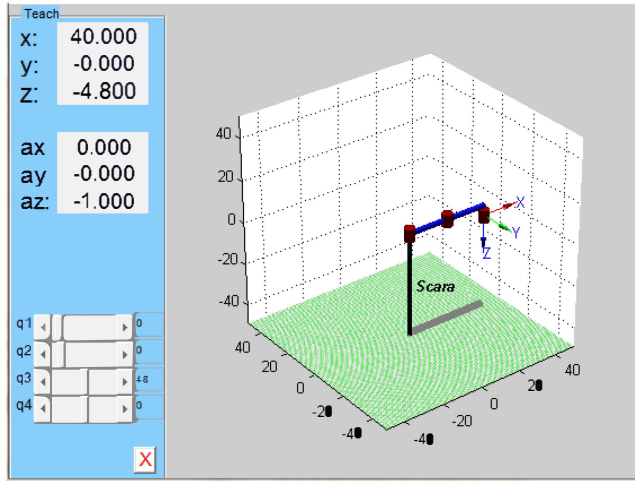


Fig. 3: Simulation model of the SCARA robot

## IV. PATH PLANNING

### 1. Path planning in joint space

The final pose can be solved by using the inverse kinematic while the initial pose is known, however, the path planning of each joint need calculate, respectively. Assumed a joint has an initial angle  $\theta_i$ , when the motions begin and the final angle  $\theta_f$  is in the motions end. If the joint motions during the rotation need to be smooth, at least 4 constraints of the joints trajectory functions are required. Meanwhile, assumed  $V_i$  and  $V_f$  are velocity of the joint at the begin and the end of the motion, then a unique cubic polynomial (12) can be solved by using the constraints mentioned above. Equation (13) is the solution of (12).

$$\theta(t) = c_0 + c_1 t + c_2 t^2 + c_3 t^3 \quad (12)$$

$$\begin{cases} c_0 = \theta_i \\ c_1 = v_i \\ c_2 = -\frac{3\theta_i - 3\theta_f + 2v_i t + v_f t}{t^2} \\ c_3 = \frac{2\theta_i - 2\theta_f + v_i t + v_f t}{t^3} \end{cases} \quad (13)$$

In practice, the cubic polynomial will cause mutation of acceleration. To solve this problem, the acceleration of the motion should also be constrained. Assumed  $a_i$  and  $a_f$  are acceleration of the joint at the begin and the end of the motion, then a unique quintic polynomial equation can be obtained as

$$\theta(t) = c_0 + c_1 t + c_2 t^2 + c_3 t^3 + c_4 t^4 + c_5 t^5 \quad (14)$$

$$\begin{cases} c_0 = \theta_i \\ c_1 = v_i \\ c_2 = \frac{a_i}{2} \\ c_3 = \frac{[20\theta_f - 20\theta_i - (8v_f + 12v_i)t_f - (3a_i - a_f)t_f^2]}{2t_f^3} \\ c_4 = \frac{[30\theta_i - 30\theta_f + (14v_f + 16v_i)t_f - (3a_i - 2a_f)t_f^2]}{2t_f^4} \\ c_5 = \frac{[12\theta_f - 12\theta_i - (6v_f + 6v_i)t_f - (a_i - a_f)t_f^2]}{2t_f^5} \end{cases} \quad (15)$$

### 2. Path planning in Cartesian space

In most situations, the path of end effector is required to a specific curve. For example, the motion path of the end effector should be a straight line or arc line, when the initial point and end point is known. The interpolation method can achieve this purpose. Equation (16) can be used to transform Cartesian coordinate to joint coordinate, if all the interpolating points are in task space.

$$\begin{cases} \theta_1 = \pi - \arccos\left(\frac{l_1^2 + l_2^2 - (x^2 + y^2)}{2l_1 l_2}\right) \\ \theta_2 = \arctan\left(\frac{y}{x}\right) - \arctan\left(\frac{l_2 \sin(\theta_1)}{l_1 + l_2 \cos(\theta_1)}\right) \end{cases} \quad (16)$$

## V. POSITION CONTROL

This section clarifies how to calibrate workpiece by the camera. In Visual C++ Compiler Environment, OpenCV has been installed to perform the camera calibration and image process.

In computer vision, it is meaningful to confirm the relationship between real location and image of the workpiece. For this goal, the geometry model of the camera is needed. It contains internal camera parameters and extrinsic camera parameters. Zhang Zheng-you method is adopted to calibrate the camera. The calibration results are given as

$$M_1 = \begin{bmatrix} 703.6503 & 0 & 320.9820 & 0 \\ 0 & 701.5517 & 287.6760 & 0 \\ 0 & 0 & 1 & 0 \end{bmatrix} \quad (17)$$

$$M_2 = \begin{bmatrix} 0.0026 & 0.9998 & 0.0195 & 97.9088 \\ 1 & -0.0025 & 0.0069 & -26.6459 \\ 0.0069 & 0.0195 & -0.9998 & -27.6573 \\ 0 & 0 & 0 & 1 \end{bmatrix} \quad (18)$$

Fig. 4 depicts the flowchart of the position control method. The flow chart is the workflow of pick up workpiece. All of the procedure is performed on control software designed by Visual C++ 6.0 environment.

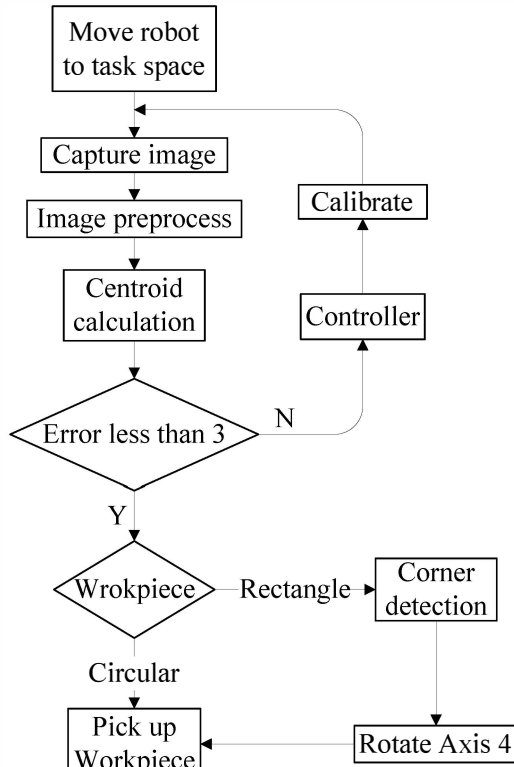


Fig. 4: Flowchart of the position control

## VI. EXPERIMENTAL RESULTS

Tables 3 and 4 list the experimental results of the circular and rectangle workpieces, respectively. The workpiece is needed 3 times to calibration generally. The desired centroid is the centroid of the workpieces in the camera coordinate, when the workpiece is placed under the electromagnet clamp. As the number of the calibration is increased, the absolute errors of  $X$  and  $Y$  positioning are decreased. The absolute errors of positioning for the circular and rectangle workpieces are satisfying, which are less than 3 pixels and 1 pixel, respectively.

**Table 3: Experimental result of the circular workpiece**

Calibration times	Desired Centroid	Actual Centroid	X absolute error	Y absolute error
1	(261,80)	(182,264)	79	180
2	(261,80)	(269,85)	8	5
3	(261,80)	(264,81)	3	1

**Table 4: Experimental result of the rectangle workpiece**

Calibration times	Desired Centroid	Actual Centroid	X absolute error	Y absolute error
1	(246,204)	(181,380)	65	176
2	(246,204)	(241,203)	5	1
3	(246,204)	(245,203)	1	1

## VII. CONCLUSION

A 4-DOF SCARA robot with 3R1P has been developed in this paper. The kinematic model, the straight line path and arc line path, the visual servo, and the experimental results of the robot have been presented. Experimental results demonstrate that the robot can calibrate the workpieces with less than 3 pixels error for the circular and rectangle workpieces, and the developed robot is feasible and valid.

## ACKNOWLEDGMENT

The authors would like to thank the National Natural Science Foundation of China under Grant NSFC51275312, the National Key Technology R&D Program under Grant 2014BAH23F04, and Shenzhen Government Fund under Grant JSGG20141015153303491 and KC2014JSJS025A.

## REFERENCES

- [1] L. E. G. Moctezuma, A. Lobov and J. L. M. Lastra, "Free Shape Paths in Industrial Robots", IECON 2012 - 38th Annual Conference on IEEE Industrial Electronics Society, 25-28 Oct 2012, pp. 3739-3743
- [2] H. Chen and Y. Liu, "Robotic assembly automation using robust compliant control", Robotics and Computer-Integrated Manufacturing, Vol. 29, No. 2, 2013, pp.293-300
- [3] C. Pop, S. M. Grigorescu and A. Davidescu, "Colored object detection algorithm for visual-servoing application", Optimization of Electrical and Electronic Equipment (OPTIM), 24-26 May 2012, pp. 1539-1544
- [4] L. U. Odhner and A. M. Dollar, "The Smooth Curvature Model: An Efficient Representation of Euler-Bernoulli Flexures as Robot Joints", IEEE Transactions on Robotics, Vol. 28, No.4, 2012, pp. 761-772
- [5] M. A. Pérez and M. Bueno, "3D Visual Servoing Control for Robot Manipulators Without Parametric Identification", IEEE Latin America Transactions, Vol. 13, No. 3, 2015, pp. 569-577
- [6] Y. Li and S. S. Ge, "Human-Robot Collaboration Based on Motion Intention Estimation", IEEE/ASME Transactions on Mechatronics, Vol. 19, No. 3, 2014, pp. 1007-1014
- [7] L. M. Capisani and A.F. Ferrara, "Trajectory Planning and Second-Order Sliding Mode Motion/Interaction Control for Robot Manipulators in Unknown Environments", IEEE Transactions on Industrial Electronics, Vol. 59, No. 8, 2012, pp. 3189-3198
- [8] D. Manocha and J. F. Canny, "Efficient inverse kinematics for general 6R manipulators", IEEE Transactions on Robotics and Automation, Vol. 5, No. 10, 1994, pp. 648-658
- [9] P. I. Corke, "A Robotics Toolbox for Matlab", IEEE Robotics and Automation Magazine, Vol.3, No.1, 1996, pp. 24-32
- [10] D. Martins and R. Guenther, "Hierarchical kinematic analysis of robots", Mechanism & Machine Theory, Vol. 38, No. 6, 2003, pp. 497-518

## BIOGRAPHIE



**Wen-Bo Li** received his B.Sc. degree from Shenzhen University in 2015.

He is currently a postgraduate with College of Mechatronics and Control Engineering, Shenzhen University, Shenzhen. His research direction is motor control.



**Guang-Zhong Cao** received the B.Sc., M.Sc., and Ph.D. degrees in electrical engineering and automation from Xi'an Jiaotong University, Xi'an, Shanxi, China, in 1989, 1992, and 1996, respectively.

He is currently a Professor and Director with the Shenzhen Key Laboratory of Electromagnetic Control, Shenzhen University, Shenzhen, Guangdong, China. He has published more than 80 articles in refereed journals and conferences. His research interests include motor control, and

control theory and its application.



**Xiao-Qin Guo** received the B.Sc., M.Sc. degree in electrical engineering and automation from Northwestern polytechnical University Shanxi Province, China.

She is currently an associate professor with College of Mechatronics and Control Engineer, Shenzhen University. She has published over 30 papers in refereed Journals and conferences. Her research interests are control theory and its application, robot and computer vision.



**Su-Dan Huang** received the B.Sc. and M.Sc. degrees in College of Mechatronics and Control Engineering from Shenzhen University, Shenzhen, Guangdong, China, in 2009 and 2012, respectively.

She is currently a joint PHD candidate with the Department of Electrical Engineering, Southwest Jiaotong University, Chengdu, Sichuan, China, and Shenzhen Key Laboratory of Electromagnetic Control, Shenzhen University, Shenzhen, Guangdong, China. Her research interests include design and control of planar switched reluctance motors, and control theory and its application.